



Higgs boson physics and broken flavor symmetry – LHC phenomenology[☆]

Edmond L. Berger^a, Hao Zhang^b

^aHigh Energy Physics Division, Argonne National Laboratory, Argonne, IL 60439, USA

^bDepartment of Physics, University of California, Santa Barbara, CA 93106, USA

Abstract

The LHC implications are presented of a simplified model of broken flavor symmetry in which a new scalar (a flavon) emerges with mass in the TeV range. We summarize the influence of the model on Higgs boson physics, notably on the production cross section and decay branching fractions. Limits are obtained on the flavon φ from heavy Higgs boson searches at the LHC at 7 and 8 TeV. The branching fractions of the flavon are computed as a function of the flavon mass and the Higgs-flavon mixing angle. We explore possible discovery of the flavon at 14 TeV, particularly via the $\varphi \rightarrow Z^0 Z^0$ decay channel in the $2\ell 2\ell'$ final state, and through standard model Higgs boson pair production $\varphi \rightarrow hh$ in the $b\bar{b}\gamma\gamma$ final state. The flavon mass range up to 500 GeV could be probed down to quite small values of the Higgs-flavon mixing angle with 100 fb^{-1} of integrated luminosity at 14 TeV.

Keywords: Higgs boson, broken flavor symmetry, flavon, Higgs-flavon mixing, LHC phenomenology

1. Introduction

The standard model (SM) of particle physics describes physics at the electroweak symmetry breaking (EWSB) scale of the visible sector remarkably well. Following the discovery of a narrow state with mass near 125 GeV, whose properties are much like those expected of the SM Higgs boson, all of the expected SM particles can be said to have been detected. Attention has turned to precise determination of the properties of this Higgs boson, notably its decay branching fractions, and to a more detailed exploration of physics at the electroweak scale, including the search for possible new physics beyond the SM.

The flavor structure of the SM remains a puzzle, and it is intriguing to consider how broken flavor symmetry may be related to broken electroweak symmetry. The fact that no significant deviations from SM predictions have appeared in flavor-related physics processes indicates that any TeV scale new physics (NP) does

not introduce an important new source of flavor change or CP violation beyond the SM. This inference hints at flavor symmetry (horizontal symmetry) in a NP model. The idea that the NP interactions are invariant under a flavor symmetry group is known as minimal flavor violation (MFV) [1]. In the MFV scenario, the SM flavor symmetry is broken explicitly by the non-vanishing SM Yukawa coupling constants. The flavor symmetry could nevertheless be a true symmetry of nature at some high energy scale but be broken by non-zero vacuum expectation values (vev's) of scalar fields called flavons.

In this report, we describe the implications for Large Hadron Collider (LHC) experiments of a simplified model of broken gauged flavor symmetry published recently [2]. The minimal new particle content of the model includes a scalar flavon, a gauge singlet under the SM; a heavy fermion T partner of the top quark; and a neutral top-philic gauge boson Z_T . The mass of the flavon could be at the TeV scale. We concentrate here on the modifications of Higgs boson production and decay properties introduced by this model and on flavon phenomenology at the LHC, notably its production cross section and the decay modes $\varphi \rightarrow hh$ and $\varphi \rightarrow ZZ$.

[☆]Paper presented by E L Berger at the 37th Conference on High Energy Physics, July 2 - 9, 2014, Valencia, Spain.

2. Simplified model of broken flavor symmetry

A “minimal” model of broken flavor symmetry was proposed in [3], and we adopted this approach as our starting point. This model has exotic fermion partners of the SM quarks, flavor gauge bosons, and two scalar flavon fields Y_u and Y_d for the up-like and down-like quarks. The large hierarchy between the masses of the SM quarks corresponds to a large hierarchy between the vevs of the flavons which suggests that the flavor symmetry could be broken sequentially [4]. If we integrate out the heavy degrees of freedom associated with the first and second generations, we are left with a simplified flavor symmetry model with a manageable number of beyond-the-SM (BSM) degrees of freedom (a flavon, an exotic fermion, and a massive vector boson) associated with the top-quark and bottom-quark sectors. Because the vev of the flavon associated with the bottom-quark is nearly two orders of magnitude larger than the vev of the flavon associated with the top-quark, we also integrated out the flavon associated with the bottom-quark. At the TeV scale, we are left with the effective Lagrangian

$$\mathcal{L}_{\text{topflavor}} = \lambda \bar{Q}_L \tilde{H} \Psi_{tR} - \lambda' \bar{\Psi}_t \Phi \Psi_{tR} - M \bar{\Psi}_t t_R + \text{h.c.} \quad (1)$$

Here Φ is a complex flavon associated with the top-quark; Q_L is the SM quark field, Ψ_t and Ψ_{tR} are the top-partner fermion fields; H is the SM Higgs doublet field, and $\tilde{H}_i \equiv \varepsilon_{ij} H_j$ where ε_{ij} is the anti-symmetric tensor with $\varepsilon_{12} = 1$. λ and λ' are dimensionless parameters, M is a parameter with the dimensions of mass.

After electroweak symmetry breaking and flavor symmetry breaking,

$$H = \begin{pmatrix} 0 \\ \frac{v + \tilde{h}}{\sqrt{2}} \end{pmatrix}, \quad (2)$$

$$\Phi = \frac{\tilde{\varphi} + v_\varphi}{\sqrt{2}}, \quad (3)$$

in the unitary gauge, where $v = 246$ GeV is the vev of the Higgs field, \tilde{h} is the physical degree of freedom of the SM Higgs doublet field, and $\tilde{\varphi}$ is the physical degree of freedom of the top flavon. The mass eigenstates (h, φ) of the scalar fields are linear combinations of \tilde{h} and $\tilde{\varphi}$:

$$\begin{pmatrix} \tilde{h} \\ \tilde{\varphi} \end{pmatrix} = \begin{pmatrix} \cos \theta_H & \sin \theta_H \\ -\sin \theta_H & \cos \theta_H \end{pmatrix} \begin{pmatrix} h \\ \varphi \end{pmatrix}, \quad (4)$$

where θ_H is the Higgs-flavon “mixing” angle. The mixing term, even if forbidden artificially at tree-level, will be generated through loop corrections. The deviation

of the Higgs field self-interaction strength λ_H from its value $\lambda_H^{SM} = m_h^2/v^2$ in the SM can be written as

$$\lambda_H \equiv \lambda_H^{SM} + \frac{m_\varphi^2 - m_h^2}{v^2} \sin^2 \theta_H. \quad (5)$$

To simplify notation, we use $c_H \equiv \cos \theta_H$ and $s_H \equiv \sin \theta_H$.

The influence of the new physics discussed here on the SM electroweak precision observables can be described with the oblique parameters S, T, U [5]. The contribution from the exotic real scalar boson φ to the oblique parameters [6] is suppressed by the mixing angle θ_H . We showed the one standard deviation (1σ), 2σ and 3σ fit regions in Ref. [2]. A detailed analysis of $\Delta F = 2$ flavor physics observables and of $B \rightarrow X_s \gamma$ in this model was presented in Ref. [7].

3. Modifications of Higgs boson physics

The interactions between the SM-like Higgs boson and other SM particles are different from those in the pure SM. The differences have two origins. First, there is mixing between the $SU(2)_L$ doublet and the flavon. Second, there is mixing between the SM top-quark and the heavy fermion T . We investigated the production cross section and the decay properties of the SM-like Higgs boson h in this gauged broken flavor symmetry model.

Gluon fusion is the most important production channel of the SM Higgs boson at the LHC. In the NP model, the interaction between the SM-like Higgs boson and the gluon is mediated by both the SM top-quark and the heavy fermion T . Denoting the SM and the NP hgg interactions as

$$c_{hgg}^{SM} h G_{\mu\nu}^a G^{\mu\nu,a}, \quad c_{hgg}^{NP} h G_{\mu\nu}^a G^{\mu\nu,a}, \quad (6)$$

respectively, we obtained

$$\begin{aligned} \frac{c_{hgg}^{NP}}{c_{hgg}^{SM}} &\rightarrow \frac{\lambda v c_H}{\sqrt{2}} \left(\frac{c_{LSR}}{m_t} - \frac{s_{LCR}}{m_T} \right) \\ &\quad - \frac{\lambda' v s_H}{\sqrt{2}} \left(\frac{s_{LSR}}{m_t} + \frac{c_{LCR}}{m_T} \right) \\ &= c_H, \end{aligned} \quad (7)$$

in the limit of large fermion mass ($m_{t,T} \gg m_h$).

We showed that the strengths of most of the Higgs coupling vertices are just rescaled by a factor c_H . We examined the loop induced interactions also. The hgg and $h\gamma\gamma$ vertices are rescaled by the factor c_H in the heavy fermion limit. The $hZ^0\gamma$ vertex deviates from the simple c_H rescaling, but the deviation is small. The Higgs

boson decay branching ratios are nearly unchanged relative to the SM since every sizable partial width is changed by an overall factor c_H^2 .

In the model, the inclusive Higgs production cross section is suppressed by a factor c_H^2 , allowed by the LHC data at 7 and 8 TeV. The result from a fit of the Higgs boson inclusive cross section $\mu = \sigma/\sigma_{SM}$ by the CMS collaboration [8] is

$$\mu = 0.80 \pm 0.14. \quad (8)$$

The result from the ATLAS collaboration

$$\mu = 1.30 \pm 0.12(\text{stat})_{-0.11}^{+0.14}(\text{sys}). \quad (9)$$

would exclude most of the parameter space of the NP model [9]. However, at the 3σ C.L., the region $s_H^2 < 0.2$ is still allowed.

4. Flavan phenomenology at the LHC

The flavon is produced dominantly through gluon fusion at the LHC. When the flavon is heavy, the heavy fermion limit is not a good approximation, and, therefore, the naively expected suppression factor s_H^2 is not valid. We calculated the flavon production cross section using the complete expressions found in Ref. [2]. In contrast to the gluon fusion case, the flavon cross sections in the VBF and vector boson associated production channels, where loop effects do not play a role, are just rescaled by a factor of s_H^2 relative to the Higgs boson cross sections.

The flavon has the same decay modes as the SM Higgs boson. For a light flavon ($m_\varphi < 2m_t$), the partial decay widths of the regular decay channels (except $\varphi \rightarrow gg, \gamma\gamma, \gamma Z$) are all rescaled by a factor of s_H^2 which will not affect the decay branching ratios of the flavon. In addition, the $\varphi \rightarrow hh$ decay width is important, and, for a relatively heavy flavon ($2m_t < m_\varphi < m_t + m_T$), the $\varphi \rightarrow t\bar{t}$ decay width. Since there is no s_H^2 suppression in the $\varphi t\bar{t}$ vertex, the flavon will decay into $t\bar{t}$ with a large branching ratio at small s_H if allowed by phase space. However, the flavon production cross section is highly suppressed by s_H^2 in this region. The signal will be hidden under the SM $t\bar{t}$ background making the signal for the flavon hard to find in this mode.

For a heavy flavon, as noted before, the heavy fermion limit is not a good approximation. We calculated the branching ratios of the loop-induced processes ($\gamma\gamma, gg, Z^0\gamma$) using the exact formula. For $m_\varphi > 160$ GeV, the contribution from the loop induced channels is negligibly small, and the most important decay modes

are $b\bar{b}, t\bar{t}, W^+W^-, Z^0Z^0$, and hh . The branching ratios for the dominant decay channels are shown in Fig. 1; $\varphi \rightarrow hh$ is an important decay channel of the flavon, and it might be used for discovery. Searches at the LHC can focus on the SM Higgs-like decay channels (Z^0Z^0, W^+W^-) and on the light Higgs boson pair decay channel.

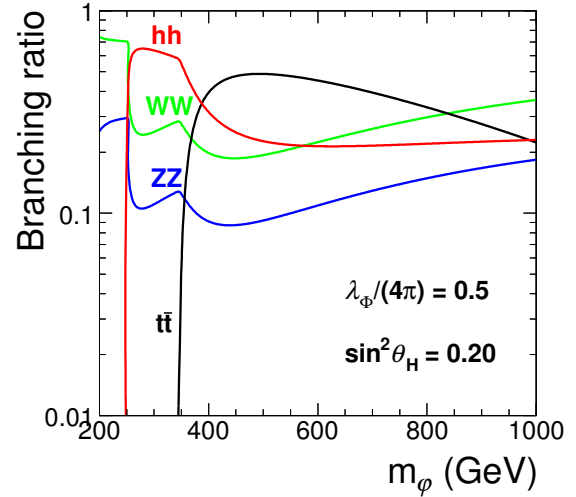


Figure 1: The decay branching ratios of the most important φ decay channels.

At 7 and 8 TeV, the strongest limit on the flavon is provided by the $Z^0Z^0 \rightarrow 2\ell 2\ell'$ channel in heavy SM Higgs boson searches [10, 11]. The CMS collaboration also investigated the hh channel [12, 13]. Limits from the 7 and 8 TeV LHC data are presented in Ref. [2].

4.1. Flavan searches at 14 TeV

We investigated the possibility of discovering a flavon at 14 TeV with 100 fb^{-1} integrated luminosity. There are simulations of the Z^0Z^0 channel by the ATLAS collaboration [14] and the CMS collaboration [15] for this channel. We rescaled their upper bounds to 100 fb^{-1} integrated luminosity. When $m_\varphi < 2m_h$, the Z^0Z^0 channel can provide a very strong constraint on the NP model (e.g., s_H^2 greater than ~ 0.08 is excluded). When $m_\varphi > 2m_h$, the constraint on s_H^2 is at $O(10^{-1})$. In this region of s_H^2 , the hh channel will be the dominant decay channel of φ . We focus on the $b\bar{b}\gamma\gamma$ channel and present the results of our detailed simulation of the signal and backgrounds.

We generated the signal and background events at the parton level using MadGraph5 [16, 17]. For signal

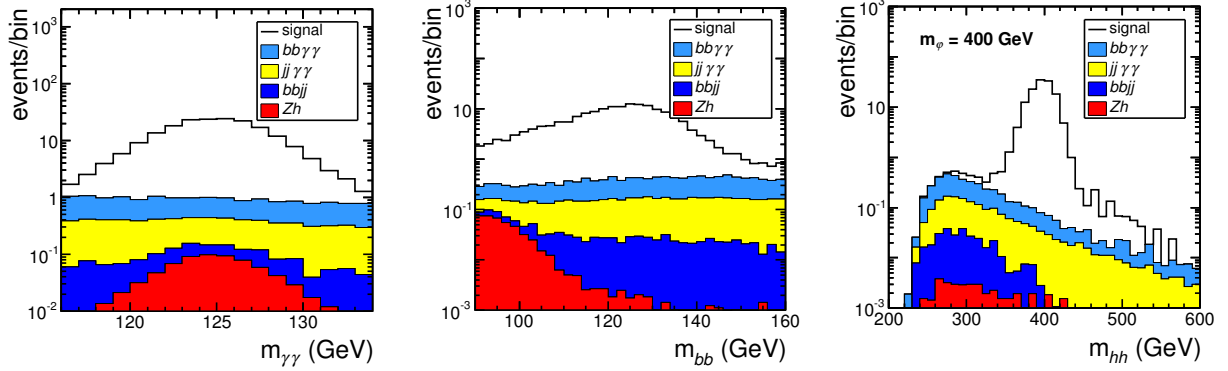


Figure 2: The reconstructed diphoton, $b\bar{b}$, and hh mass distributions are shown at 14 TeV with 100 fb^{-1} integrated luminosity. We choose $m_\varphi = 400 \text{ GeV}$. The total cross section is rescaled to the value of the SM like Higgs boson with the same mass. The decay branching ratio $\text{Br}(\varphi \rightarrow hh)$ is set to be 100%. Note that the horizontal scale differs in the three distributions.

events, we generated $pp \rightarrow \varphi + n j$ to $n=1$. All of the parton level signal and the background events were showered using Pythia6.4 [18]. The MLM matching scheme [19] was used to avoid double counting. Detector effects were mimicked with PGS4 [20]. Jets were defined in the events with the anti- k_T algorithm, with $R = 0.4$. The cross section for the signal was normalized to the NNLO SM-like Higgs boson cross section suggested by the LHC Higgs Cross Section Working Group [21] multiplied by the rescaling factor from the $gg\varphi$ vertex.

There are several irreducible SM backgrounds

$$\begin{aligned} pp &\rightarrow b\bar{b}\gamma\gamma, \\ pp &\rightarrow Z^0 h \rightarrow b\bar{b}\gamma\gamma, \\ pp &\rightarrow Z^0 \gamma\gamma \rightarrow b\bar{b}\gamma\gamma, \end{aligned} \quad (10)$$

and reducible SM backgrounds

$$\begin{aligned} pp &\rightarrow b\bar{b}jj \ (j \rightarrow \gamma), \\ pp &\rightarrow jj\gamma\gamma \ (j \rightarrow b), \\ pp &\rightarrow t\bar{t} \rightarrow bj\bar{b}jj \ (j \rightarrow \gamma), \\ pp &\rightarrow t\bar{t}h \rightarrow b\ell^+ \bar{v}\bar{\ell}^- \bar{v}\gamma\gamma \ (\ell^\pm \text{ missed}). \end{aligned} \quad (11)$$

Next-to-leading order contribution were included where available, with K factors if necessary.

We required the events to have at least two hard isolated photons in the central region,

$$p_T^\gamma > 20 \text{ GeV}, \quad |\eta^\gamma| < 2.0, \quad (12)$$

and no hard jet or charged lepton in the $\Delta R = 0.4$ region around the photon. We demanded at least two hard b -tagged jets with

$$p_T^j > 40 \text{ GeV}, \quad |\eta^j| < 2.0. \quad (13)$$

The average b -tagging efficiency was reweighted to 70% [22] in the analysis. To suppress the SM $t\bar{t}h$ background, we rejected events which contained hard isolated charged leptons and events with large missing transverse energy $\cancel{E}_T > 30 \text{ GeV}$.

Signal events were required to satisfy hard cuts designed for the Higgs boson pair signal, with cuts on the leading and sub-leading photon:

$$|m_{\gamma\gamma} - 125.4 \text{ GeV}| < \Delta m_{h,\text{cut}}^{\gamma\gamma}. \quad (14)$$

The transverse momentum of the leading and of the sub-leading photon had to satisfy

$$p_T^{\gamma_1} > p_{T,\text{cut}}^{\gamma_1}, \quad p_T^{\gamma_2} > p_{T,\text{cut}}^{\gamma_2}. \quad (15)$$

The leading and sub-leading b -tagged jets had to satisfy

$$|m_{bb} - 125.4 \text{ GeV}| < \Delta m_{h,\text{cut}}^{bb}. \quad (16)$$

$\delta\phi_{\gamma b}$, the smallest of $\Delta\phi_{\gamma_1 b_1}$, $\Delta\phi_{\gamma_1 b_2}$, $\Delta\phi_{\gamma_2 b_1}$, $\Delta\phi_{\gamma_2 b_2}$ (the differences between the azimuthal angles of the objects) was required to be less than $\Delta\phi_{\gamma b}$.

We reconstructed the invariant mass peak of the flavon after including the energy resolution. In Fig. 2, we show the results for the reconstructed diphoton, $b\bar{b}$, and hh mass distributions using events which satisfy all the cuts. The resonance signal is clear. The dominant background is $b\bar{b}\gamma\gamma$, and the other backgrounds are numerically small. The diphoton resonance is very clear; the $b\bar{b}$ peak is wide owing to the larger energy smearing of jets.

After a scan over the mass of the flavon, we derived expected limits from the search for the $\varphi \rightarrow hh \rightarrow b\bar{b}\gamma\gamma$ signal at 14 TeV with 100 fb^{-1} . These limits can be

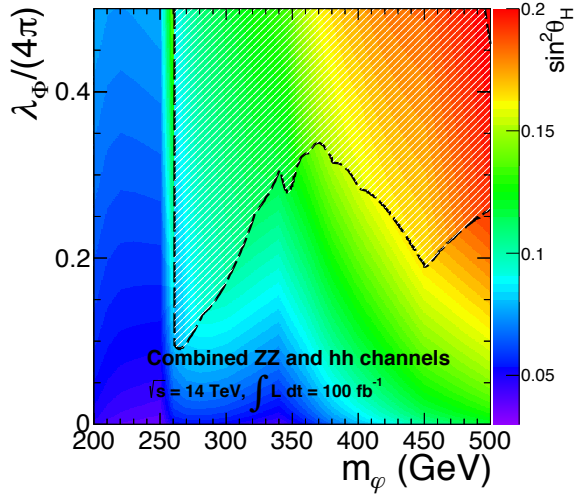


Figure 3: Combination of the 2σ exclusion region of s_H^2 results for the $\varphi \rightarrow Z^0 Z^0 \rightarrow 2\ell 2\ell'$ search and the $\varphi \rightarrow hh \rightarrow b\bar{b}\gamma\gamma$ search. In the upper part of the figure, in the irregularly shaped region above the broad-dashed line, the $\varphi \rightarrow hh \rightarrow b\bar{b}\gamma\gamma$ search yields a stronger constraint.

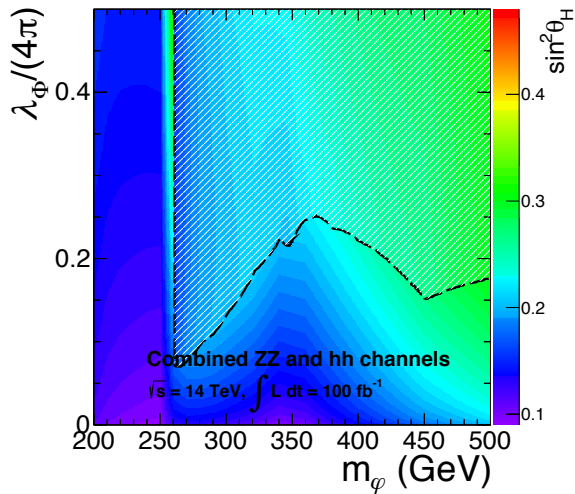


Figure 4: The 5σ discovery significance of the required value of s_H^2 from a combination of the $\varphi \rightarrow Z^0 Z^0 \rightarrow 2\ell 2\ell'$ search and the $\varphi \rightarrow hh \rightarrow b\bar{b}\gamma\gamma$ search. In the upper part of the figure, in the irregularly shaped region above the broad-dashed line, the $\varphi \rightarrow hh \rightarrow b\bar{b}\gamma\gamma$ process is more sensitive to the NP model.

translated into a constraint on the NP parameters. Combining the results from the SM-like heavy Higgs boson search for $\varphi \rightarrow Z^0 Z^0$ and the $\varphi \rightarrow hh \rightarrow b\bar{b}\gamma\gamma$ search

at 14 TeV with 100 fb^{-1} integrated luminosity, we show the constraint on s_H^2 in Fig. 3. The combined 5σ discovery significance is shown in Fig. 4. In FIG. 3, the search for the $\varphi \rightarrow hh \rightarrow b\bar{b}\gamma\gamma$ signal gives a stronger constraint in the cross-hatched region. This signal can give a stronger constraint in the large λ_ϕ region when the $\varphi \rightarrow hh$ channel opens. This figure shows that a strong constraint on the neutral scalar φ can be obtained with a combination of the two channels.

5. Summary

A model of physics beyond the SM has been proposed in which there is a new scalar, a flavon, a new heavy fermion associated with the SM top-quark, and a new neutral flavor gauge boson. This model arises as the low-energy limit of a theory of gauged flavor symmetry with an inverted hierarchy, giving a simplified model with spontaneous breaking of flavor symmetry. The flavon mixes with the SM Higgs boson, and the heavy fermion alters the production and decay properties of the Higgs boson at the LHC, all in ways that are consistent with data at current levels of precision. The flavon and the heavy fermion might appear at the hundreds of GeV to the TeV scale. There is a sizable allowed parameter space in which existing constraints from electroweak precision observables and flavor physics are satisfied.

In this NP model, the production cross section of the SM-like Higgs boson at the LHC is suppressed by a factor $\cos^2 \theta_H$, where θ_H is the mixing angle between the Higgs boson and the flavon. However, neither mixing nor the triangle loop from the heavy fermion change the Higgs boson decay branching ratios significantly. The possibility to search for the flavon at the LHC was explored in detail through its decays to a SM Higgs-pair, $\varphi \rightarrow hh$, as well as through the SM Higgs boson decay modes. At 7 and 8 TeV at the LHC, the $Z^0 Z^0$ channel will give a stronger constraint than $\varphi \rightarrow hh$ owing to limitations of integrated luminosity. At 14 TeV with 100 fb^{-1} integrated luminosity, the small mixing region can be reached where the $\varphi \rightarrow hh$ signal is important for discovery. The flavon can be produced singly at the LHC. If it decays into the hh final state with a sizable decay branching ratio, the hh cross section will be enhanced significantly by this resonance effect.

Acknowledgments. The work of E. L. Berger at Argonne is supported in part by the U.S. DOE under Contract No. DE-AC02-06CH11357. H. Zhang has been supported by the U.S. DOE under Contracts No. DE-FG02-91ER40618 and DE-SC0011702. We warmly acknowledge the essential contributions of Steven Gid-

dings, UC Santa Barbara, and Haichen Wang, LBNL, Berkeley, to the research summarized in this brief report.

References

- [1] G. D’Ambrosio, G. Giudice, G. Isidori, A. Strumia, Minimal flavor violation: An Effective field theory approach, *Nucl.Phys. B* 645 (2002) 155–187. arXiv:hep-ph/0207036, doi:10.1016/S0550-3213(02)00836-2.
- [2] E. L. Berger, S. B. Giddings, H. Wang, H. Zhang, Higgs-flavon mixing and LHC phenomenology in a simplified model of broken flavor symmetry, *Phys.Rev. D* 90 (2014) 076004. arXiv:1406.6054, doi:10.1103/PhysRevD.90.076004.
- [3] B. Grinstein, M. Redi, G. Villadoro, Low Scale Flavor Gauge Symmetries, *JHEP* 1011 (2010) 067. arXiv:1009.2049, doi:10.1007/JHEP11(2010)067.
- [4] T. Feldmann, M. Jung, T. Mannel, Sequential Flavour Symmetry Breaking, *Phys.Rev. D* 80 (2009) 033003. arXiv:0906.1523, doi:10.1103/PhysRevD.80.033003.
- [5] M. E. Peskin, T. Takeuchi, A New constraint on a strongly interacting Higgs sector, *Phys.Rev.Lett.* 65 (1990) 964–967. doi:10.1103/PhysRevLett.65.964.
- [6] V. Barger, P. Langacker, M. McCaskey, M. J. Ramsey-Musolf, G. Shaughnessy, LHC Phenomenology of an Extended Standard Model with a Real Scalar Singlet, *Phys.Rev. D* 77 (2008) 035005. arXiv:0706.4311, doi:10.1103/PhysRevD.77.035005.
- [7] A. J. Buras, M. V. Carlucci, L. Merlo, E. Stamou, Phenomenology of a Gauged $SU(3)^3$ Flavour Model, *JHEP* 1203 (2012) 088. arXiv:1112.4477, doi:10.1007/JHEP03(2012)088.
- [8] Combination of standard model higgs boson searches and measurements of the properties of the new boson with a mass near 125 gev, Tech. Rep. CMS-PAS-HIG-13-005, CERN, Geneva (2013).
- [9] Updated coupling measurements of the higgs boson with the atlas detector using up to 25 fb^{-1} of proton-proton collision data, Tech. Rep. ATLAS-CONF-2014-009, CERN, Geneva (2014).
- [10] Measurements of the properties of the higgs-like boson in the four lepton decay channel with the atlas detector using 25 fb^{-1} of proton-proton collision data, Tech. Rep. ATLAS-CONF-2013-013, CERN, Geneva (Mar 2013).
- [11] S. Chatrchyan, et al., Measurement of the properties of a Higgs boson in the four-lepton final state arXiv:1312.5353.
- [12] Search for extended higgs sectors in the h to hh and a to zh channels in $\sqrt{s} = 8 \text{ tev}$ pp collisions with multileptons and photons final states, Tech. Rep. CMS-PAS-HIG-13-025, CERN, Geneva (2013).
- [13] Search for the resonant production of two higgs bosons in the final state with two photons and two bottom quarks, Tech. Rep. CMS-PAS-HIG-13-032, CERN, Geneva (2013).
- [14] Beyond-the-standard-model higgs boson searches at a high-luminosity lhc with atlas, Tech. Rep. ATLAS-PHYS-PUB-2013-016, CERN, Geneva (2013).
- [15] Performance studies on the search for 2hdm neutral higgs bosons with the cms phase-ii detector upgrades, Tech. Rep. CMS-PAS-FTR-13-024, CERN, Geneva (2013).
- [16] J. Alwall, M. Herquet, F. Maltoni, O. Mattelaer, T. Stelzer, MadGraph 5 : Going Beyond, *JHEP* 1106 (2011) 128. arXiv:1106.0522, doi:10.1007/JHEP06(2011)128.
- [17] J. Alwall, R. Frederix, S. Frixione, V. Hirschi, F. Maltoni, et al., The automated computation of tree-level and next-to-leading order differential cross sections, and their matching to parton shower simulations arXiv:1405.0301.
- [18] T. Sjostrand, S. Mrenna, P. Z. Skands, PYTHIA 6.4 Physics and Manual, *JHEP* 0605 (2006) 026. arXiv:hep-ph/0603175, doi:10.1088/1126-6708/2006/05/026.
- [19] M. L. Mangano, M. Moretti, F. Piccinini, M. Treccani, Matching matrix elements and shower evolution for top-quark production in hadronic collisions, *J. High Energy Phys.* 0701 (2007) 013. arXiv:hep-ph/0611129, doi:10.1088/1126-6708/2007/01/013.
- [20] J. Conway, et al.[link]. URL <http://www.physics.ucdavis.edu/~conway/research/software/pgs/pgs4-olympics.htm>
- [21] S. Dittmaier, et al., Handbook of LHC Higgs Cross Sections: 1. Inclusive Observables arXiv:1101.0593, doi:10.5170/CERN-2011-002.
- [22] Performance assumptions based on full simulation of an upgraded atlas detector at a high-luminosity lhc, Tech. Rep. ATLAS-PHYS-PUB-2013-009, CERN, Geneva (2013).